We are IntechOpen,
the world's leading publisher of
Open Access books
Built by scientists, for scientists

6,900
Open access books available

186,000
International authors and editors

200M
Downloads

154
Countries delivered to

Our authors are among the

TOP 1%
most cited scientists

12.2%
Contributors from top 500 universities

CLARIVATE ANALYTICS
BOOK CITATION INDEX
INDEXED

WEB OF SCIENCE™

Selection of our books indexed in the Book Citation Index
in Web of Science™ Core Collection (BKCI)

Interested in publishing with us?
Contact book.department@intechopen.com

Numbers displayed above are based on latest data collected.
For more information visit www.intechopen.com

Nanolithography in the Evanescent Field of Noble Metals

Yong Yang[1], Guanxiao Cheng[2], Shaolin Zhou[3], Lixin Zhao[1] and Song Hu[1]
[1]Institute of Optics and Electronics, Chinese Academy of Sciences, Chengdu
[2]College of Electronic Science and Technology, Shenzhen University, Shenzhen
[3]School of Electronic and Information Engineering, South China University of Technology
Guangzhou
China

1. Introduction

With the rapid progress of high integrity in integrity circuit(IC) field, the finer resolution of optical lithography became more and more urgent which spurs the scientists to put a premium eye on resolution, throughput and reliability. According to Abbe's theory, the spatial resolution can be improved by using either shorter wavelengths or higher numerical apertures. Although the semiconductor industry has made significant progress in increasing the lithography resolution in the past decades, further improvement of the resolution by accessing shorter wavelengths is facing critical challenges due to the availability of optical materials with suitable refractive index. The expansion of nanoscale science and engineering will require flexible, high spatial resolution, and low-cost nanolithographic techniques and systems other than those employed in the semiconductor industry, for reasons of both cost and limited flexibility. So far, optical projective lithography technique is of dominance in optical lithography, resolution can be extended to $32\,nm$ or even less by using ArF light resource combined with immersion technique; however, resolution below $32\,nm$ meets great difficulty till optical lithography being washed out. According to the International Technology Roadmap for Semiconductors(ITRS2009 Edition), next generation lithography techniques for feature size $32\,nm$ and below are $193\,nm$ immersion double patterning, $193\,nm$ immersion with other fluids and lens materials, Maskless Lithography(ML2)and imprint etc., but the techniques of breaking the limitation of $32\,nm$ resolution is far from mass production; they met the difficulties of complicated fabrication procedure, low efficiency and production. A number of near-field nanolithography techniques have been explored recently by some research groups.

In the early 20th century, scientists had observed the phenomena of Surface Plasmons Polaritons（SPPs） in reflective spectrum of metallic grating. In 1902, American scientist R. W. Wood found the totally different diffraction property of light when light was introduced to metallic grating and dielectric grating. Due to the lack of reasonable explanation for such strange phenomena, his report hadn't drawn much attention from other scientists. Till 1957, American scientist R. H. Ritchie reported that the free electrons of metal surface can be resonantly excited by light, which caused the SPPs propagated

along the metallic surface. Since then, SPPs have drawn more concentrations from scientists to investigate its novel application.

With the development of microfabrication and nanotechnology, more and more attentions from scientists were paid to SPPs. T. W. Ebbesen reported the optical extraordinary transmision through subwavelength holes arrays. Leaec and his team found more details of diffraction property when light passed through subwavelength hole arrays, which will caused intensive transmission and small diffraction angle. British professor Barnes proved the reasonable existence of extraordinary transmission caused by SPPs. American scientist and his team made further experiments to prove the feasibility of super-resolution realized by SPPs metallic structure. So far, SPPs had shown its significant potential in several fields, such as optical super-resolution, bio-sensor, nano-photon devices etc..

J. Pendry predicted that a slab of negative refractive index material has the power to focus all Fourier components of a two-dimension image. According to Ebbesen's paper, SPPs are waves that propagate along the surface of a conductor, usually a metal. These are essentially light waves that are trapped on the surface because of their interaction with the free electrons of the conductor. The intensity of SPPs propagating along a smooth surface decreased due to the intrinsic absorption of metal. In order to investigate the influence of gain-assisted metamaterial in subwavelength optical lithography, we proposed a subwavelength optical lithography method based on SPPs. We computed and analyzed the distribution of optical field by the method of Finite Element Analysis (FEA). The results show that the images of object can be reconstructed by the structure.

In recent years, a flurry of activity in the fundamental research and development of surface plasmon based structures and devices were reported. The research on Nanolithography Based on Nobel Metals in this chapter is a step in the direction of providing affordable, highly flexible nanolithography. In this chapter, we present the case of nanolithography employed noble metal as objective lens to focus illumination light. The high-resolution surface plasmonic nanolithography has been investigated by using optical proximity exposure in the evanescent near field in nano-filmed noble metals. Sub-diffraction-limited feature size can be resolved by using I-line illumination exposure. And the simulations and experiments showed that sub-diffraction-limited feature size can be resolved by our given method, as illustrated in Fig. 1.
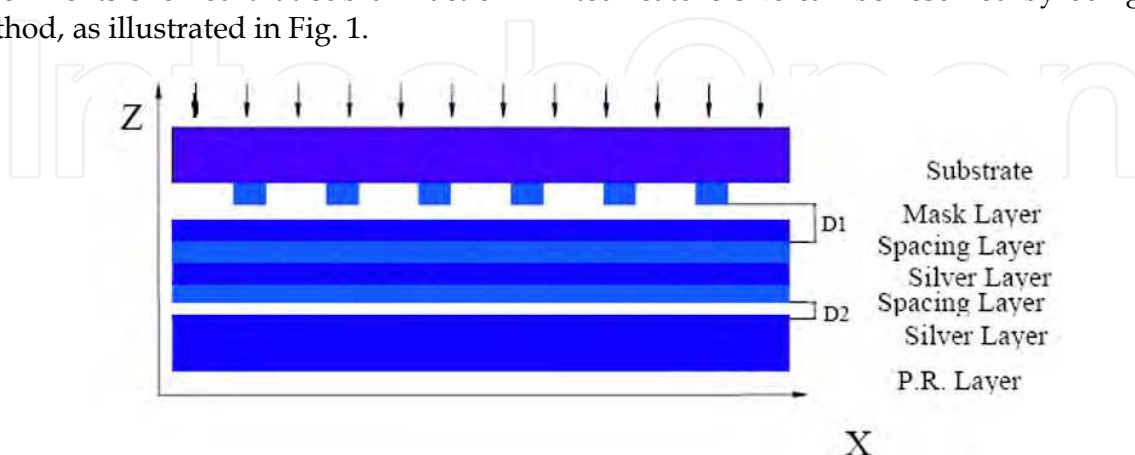
Fig. 1. Schematic of nanolithography by using noble metals. Multiple layers composing of noble metals and matched spacing imaged the mask on the photoresist layer. Patterns of arbitrary geometry on mask are reconstructed by the hetero-structure.

2. Surface plasmons plaritons

Fig. 2 shows the charges and the electromagnetic field of SPPs propagating along smooth surface. Assuming SPPs propagate along the x-axis with its propagating constant of k, the electromagnetic waves can be described by:

$$E = E_0^{\pm} \exp[+i(k_x x \pm k_z z - i\omega t)] \,, \tag{1}$$

Where, + for $z \geq 0$, - for $z \leq 0$, and with imaginary k_z, which causes the exponential decay of the field E_z. The wave vector k_x is parallel to the x direction, and

$$k_x = 2\pi / \lambda_p \,, \tag{2}$$

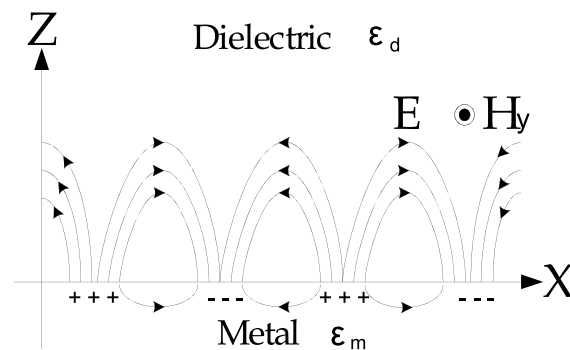where, λ_p is the wavelength of the plasma oscillation.

Fig. 2. Schematic of the charges and the electromagnetic field of SPPs propagating in the x-direction.

From Maxwell's equations and continuity at the boundary of metal and dielectric, the following dispersion relation of SPPs are derived:

$$\begin{aligned} k_x &= k_0 \sqrt{\varepsilon_m \varepsilon_d / (\varepsilon_m + \varepsilon_d)} \\ k_{zm} &= k_0 \varepsilon_m / \sqrt{\varepsilon_m + \varepsilon_d} \\ k_{zd} &= k_0 \varepsilon_d / \sqrt{\varepsilon_m + \varepsilon_d} \end{aligned} \,, \tag{3}$$

where $k_0 = 2\pi / \lambda_0$ is the wave vector of incident light in free space, k_{zm} and k_{zd} are the z component of wave vector for metal and dielectric respectively, and λ_0 is the wavelength of incident light. For any metal material, due to the metal's dispersion relation, there exists imaginary part of its permittivity which determines the skin depth of SPPs. However, the imaginary part of the dielectric can be ignored compared to the metal's imaginary part at the same incident light wavelength. So, we should shift our concentration to the imaginary part of material's permittivity.

As for the penetration of SPPs into either media, we can value it by its skin depth which was define by its field falls to $1/e$, that is

$$|z| = 1/|k_z| \,, \tag{4}$$

or in the metal medium:

$$|z_m| = \frac{2\pi}{\lambda} \sqrt{\frac{\varepsilon_{mR} + \varepsilon_d}{\varepsilon_{mR}^2}} \,, \tag{4a}$$

and in the dielectric medium:

$$|z_d| = \frac{2\pi}{\lambda} \sqrt{\frac{\varepsilon_{mR} + \varepsilon_d}{\varepsilon_d^2}} \,, \tag{4b}$$

where ε_{mR} is the real part of ε_m.

3. Nanolithography in the evanescent near field by using nano-filmed noble metal layer(s)

The sharpness of object can't be resolved by conventional lens due to the limitation by the wavelength of illumination light. J. B. Pendry had predicted that a slab of negative refractive index material has the power to focus all Fourier components of a 2D image. The super resolution of the negative index materials using silver layer, which was called 'superlens', can reconstruct the image of a pattern with line width of $40\,nm$ (Fang, et al., 2005). They made mask, silver slab and photoresist integrity in Fang's experiment, which likes the traditional contact exposure of lithography. It is not practical in real application by Fang's method of nanolithography because each wafer needs its respective mask. The experiments of super resolution using silver slab was reported, and the line width with one fifth of illumination wavelength can be successfully resolved by the silver slab (Blaikie et al., 2006).

In order to investigate the influence of distance between mask and noble metal slab on imaging, we designed a separated 'superlens' with silver slab $100\,nm$ away from mask. We analyzed the distribution of optical field by Finite Difference Time Domain (FDTD). The results show that the images of object can be reconstructed by the structure.

3.1 Nanolithography method

The exposure method of near-field nanolithography that was proposed by this paper is illustrated in Fig. 1, and the parameters of the materials are shown in Table 1. A UV transparent substrate with refractive index of n = 1.6 (@365$\,nm$) is used for supporting the mask. The object layer with line width of $60\,nm$ and pitch of $120\,nm$, which is made of Cr with refractive index of n=2.924 (@365$\,nm$), acts as the function of mask in exposure. The air gap comes from the vacuum contact between mask and silver layer, which can be viewed as a kind of practical nanolithography technique.

In Fig. 1, the spacing layer with refractive index of n=1.517 (@365$\,nm$) acts as the following two functions: 1) to match the surface plasmon polaritons resonating conditions; 2) to protect the surface of silver slab.

In order to explore the potential valid imaging distance between mask and photoresist, a repeatation of spacing layer and silver slab layer was followed after the first silver slab. The sample was exposed in i-line light that shone from the substrate side. For the convenience of

description, we defined D1 as the distance between mask and silver slab, and D2 as the distance between silver slab and photoresist, as shown in Fig. 1.

Materials	Parameters	Thickness
Substrate	n=1.6@365nm	100nm
Mask	n=2.9@365nm	40nm
Spacing	n=1.52@365nm	40nm
Silver	ε=-2.4+i*0.2488@365nm	40nm
Photoresist	n=1.7@365nm	100nm

Table 1. Physical parameters of the materials.

3.2 When silver slab separated 40 nm from mask (i.e. D1=40 nm)

In order to save calculating time and PC resources, we computed the distribution of optical near-field intensity by the 2-D FDTD method. We chose cell size of $X \times Z = 2nm \times 1nm$, which is much smaller than both the exposure light wavelength and the mask's feature size. The timestep, according to Courant condition, should be:

$$TimeStep = 2\sqrt{2}N^{1/3} \tag{5}$$

N is the total cells of computing area. We chose 3500, by which the amplitude of electric field already became steady. The distance of 40 nm comes from the spacing layer. At this situation, it is a kind of ideal condition, because mask and spacing layer had a hard contact. The surface plasmons polaritons of two interfaces between silver slab and its surroundings can magnify the evanescent waves that carried the detailed information of object. When D1=40 nm, we calculated the following four conditions: D2=0 nm, 20 nm, 40 nm, 60 nm. Fig. 3 shows the distribution of electromagnetic (abbreviated to EM afterwards in the paper) field respectively.

It was found that the image of mask can be clear resolved by the method. Fig. 3(a) shows better result, however, Fig. 3(b)-(d) showed worse results due to the exponential decay of the evanescent waves came from the exit side of the interface between silver slab and photoresist. The strong contrast of EM field may come from the edge effect of the evanescent waves. We chose the 10 nm cross-section of photoresist layer to compare the imaging result of silver slab. When D1=40 nm and D2 varied from 0 nm to 60 nm, the distribution of optical field in the section was shown in Fig. 3. When D2 changed from 0 nm to 60 nm, the amplitude reduced to about a half under the same condition, but the high contrast of lines still can be clearly observed in Fig. 4. The amplitudes of lines were relatively uniform when D_2=20 nm and 60 nm compared with D_2=0 nm. If the parameters of photoresist were under better control, the lines of images will be more uniform. However, compare with the condition of D2=0 nm, the depth of lines in photoresist will be shallower at the same exposure condition.
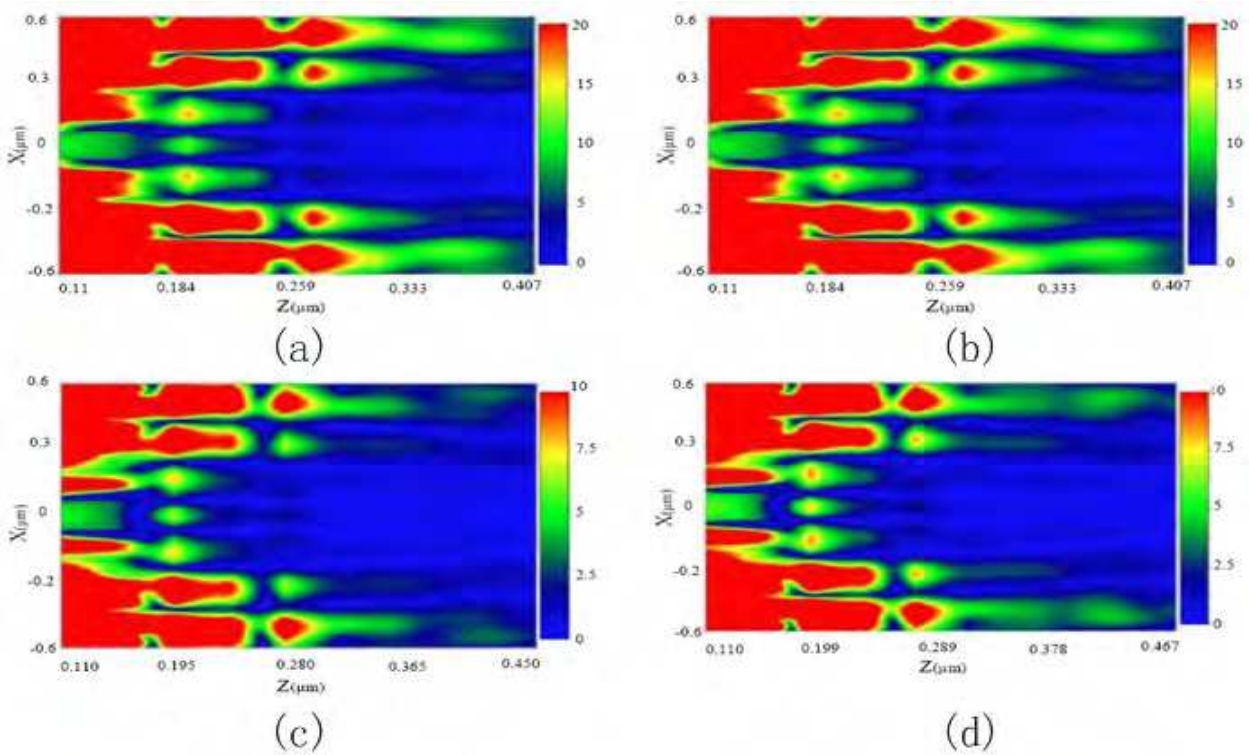
Fig. 3. The distribution of EM field in the model. Photoresist layer lies (a) between
Z=0.31 μm and Z=0.41 μm, (b) between Z=0.33 μm and Z=0.43 μm, (c) between Z=0.35 μm
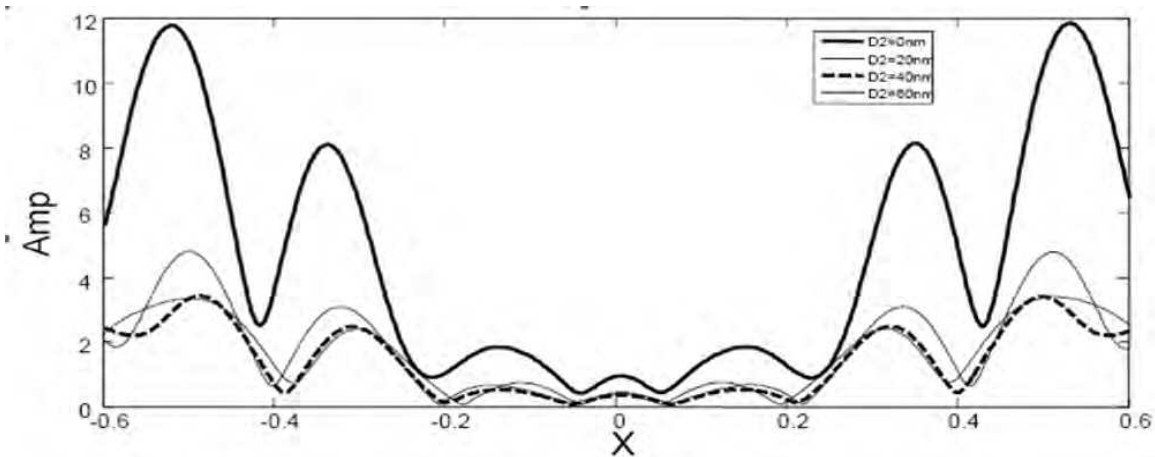and Z=0.45 μm, (d) between Z=0.7 μm and Z=0.47 μm.

Fig. 4. The distribution of optical field in the 10 nm cross-section of photoresist when
D1=40 nm.

3.3 When silver slab separated 60 nm and 80 nm from mask (i.e. D1=60 nm, 80 nm)

When D1=60 nm, 80 nm, we calculated four conditions respectively for each D1. We still
chose the 10 nm cross-section of photoresist layer to investigate the optical field. In order to
show the clear comparison results, we give the final comparison of the amplitude instead of
EM distribution figures for each condition of different D2. Fig. 5 and Fig. 6 showed the
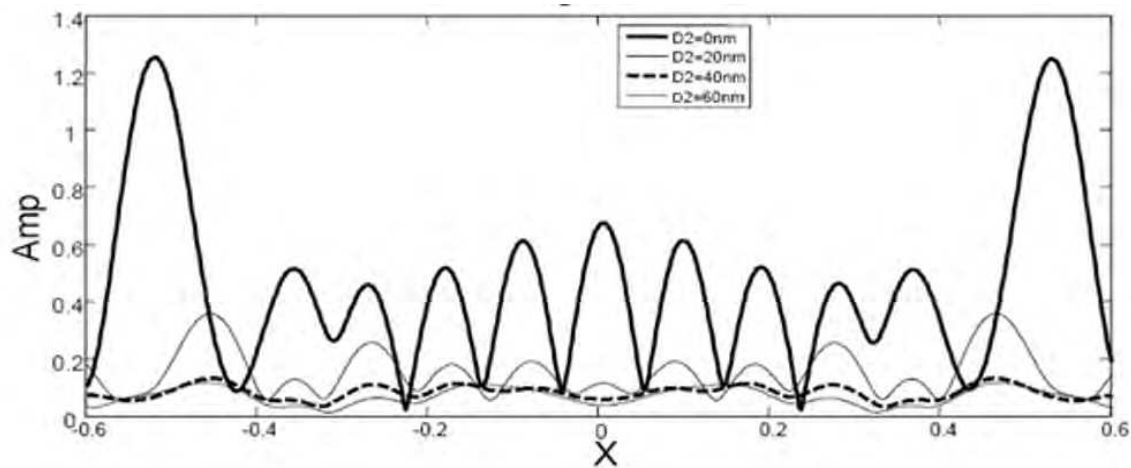result respectively when silver slab separated 60 nm and 80 nm from mask.

Fig. 5. The final comparison when D$_1$=60 nm while D$_2$=0 nm , 20 nm , 40 nm and 60 nm .
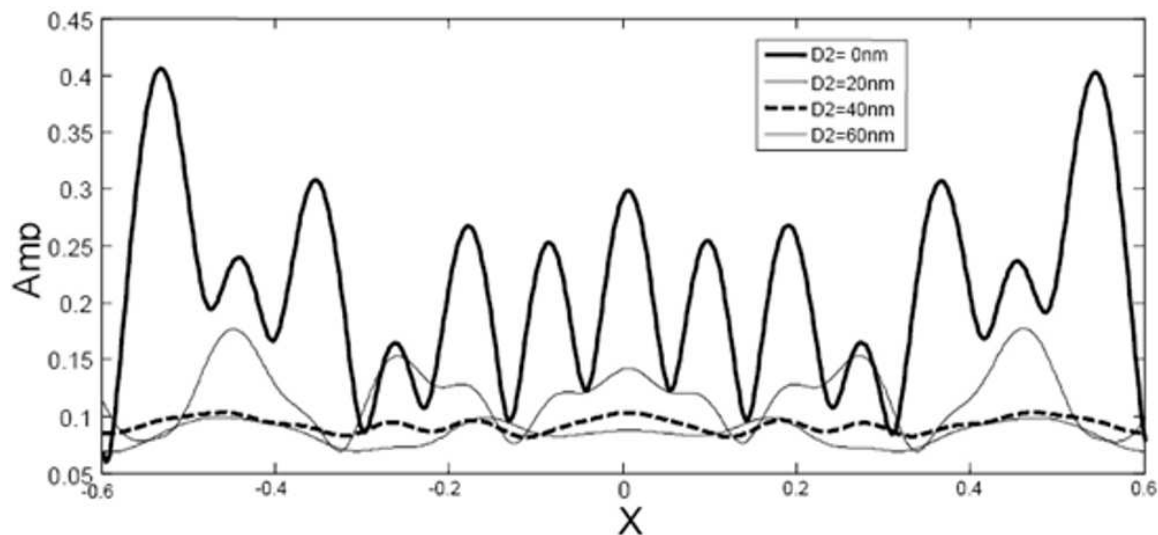

Fig. 6. The final comparison when D1=80 nm while D2=0 nm , 20 nm , 40 nm and 60 nm .

It was found that there came out extra fringes in Fig. 5 and Fig. 6. This kind of phenomena may be caused by the strong interference effects among evanescent waves. The image of mask still can be resolved in photoresist layer by proper choice of materials and exposure conditions. These results showed a bad conformity between mask and recorded image in photoresist layer. On the other hand, it gave us a hint to realize better resolution of optical lithography by reasonably using the interference effect.

3.4 When silver slab separated 100 nm from mask (i.e. D1=100 nm)

The evanescent waves cannot propagate to a long distance due to its exponential attenuation. The intensity of evanescent waves decays with a characteristic length Z_0 :

$$Z_0 = \frac{n}{k_t \sqrt{\sin^2 \theta_1 - n^2}} \tag{6}$$

where $n = n_2 / n_1$ is the relative refractive index of two surrounding media; θ_1 is the incidence angle of light from optically denser media to optically thinner media; where $k_t = 2n_2\pi / \lambda$, λ is the wavelength of incident light. Theoretically, Z_0 can be $100\,nm$ by calculation.

In order to explore the potential imaging property of silver slab, we increased D1 as much as possible. Considering the evanescent waves may diminish when $D_1=100\,nm$, so we calculated the condition of D2=$0\,nm$ only, the distribution of electromagnetic filed was shown in Fig. 7. It was found that the image of mask still can be resolved clearly in photoresist layer with good uniformity of imaged lines. We investigated the distribution of optical field in the $10\,nm$ cross-section of photoresist layer. The distribution of optical filed in the transverse section of photoresist was shown in Fig. 8. The image of mask can be resolved with high contrast. With proper choice of exposure condition and materials, the information of mask can be transferred to photoresist layer, and the image of mask can be reconstructed by the silver slab layer.
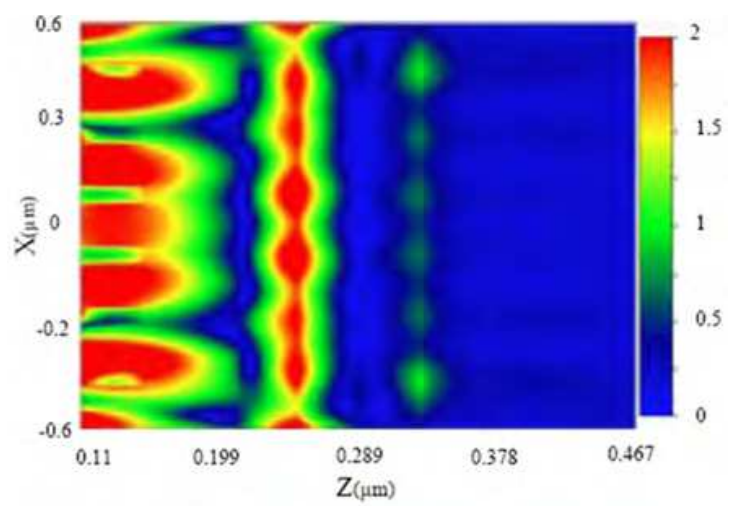

Fig. 7. The distribution of electromagnetic field in the model (Both X and Z is in unit of μm. Photoresist layer lies between Z=0.37 μm and Z=0.47 μm).
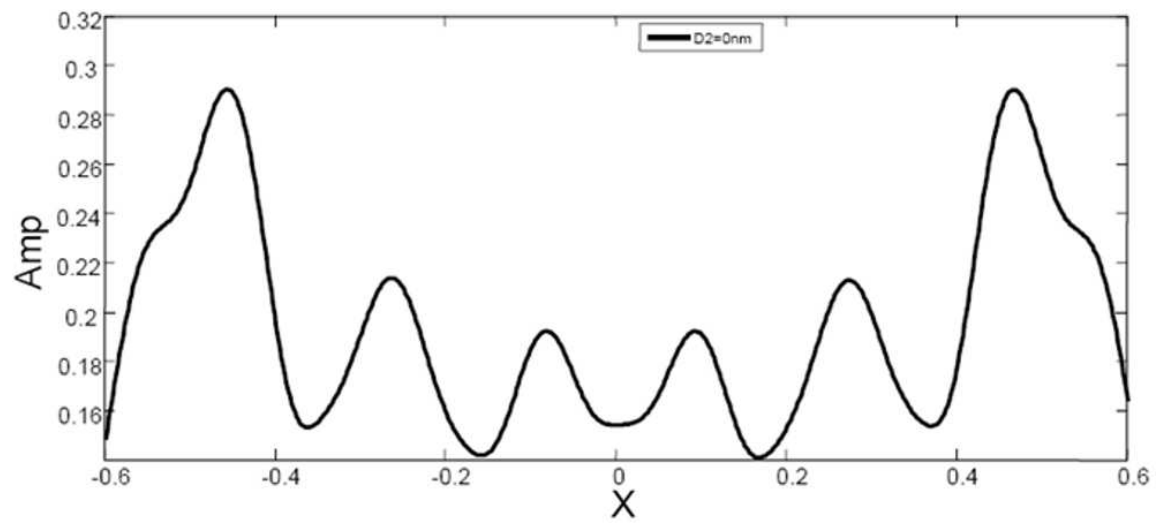

Fig. 8. The distribution of optical field in the $10\,nm$ cross-section of photoresist when silver slab separated $100\,nm$ from mask.

In brief, the image of mask can be transferred to the photoresist layer by the enhancement function of surface plasmons polaritons in silver slab. We calculated the 2D distribution of electromagnetic field in our model; the results showed that the image of mask with feature size of $60\,nm$ can be resolved in photoresist layer when silver slab separated $100\,nm$ from mask. By proper design and choice of material, nanolithography with better resolution can be realized by the very function of silver slab.

3.5 Nanolithography experiments

In order to further investigate the potential resolution of multiple layer of hetero-structure, we design a nanolithography composing of dual silver-dielectric configuration. Fig. 9 shows the distribution of electric filed in the evanescent field of nano-filmed noble metals under the illumination of i-line light. The parameters of the configuration are shown in Table 2.

Materials	Parameters	Thickness
Substrate	n=1.6@365nm	100nm
Mask	n=2.9@365nm	50nm
Spacing	n=1.52@365nm	20nm
Silver	$\varepsilon=-2.4+i*0.2488$@365nm	20nm
Photoresist	n=1.7@365nm	100nm

Table 2. Physical parameters of the materials.

For the pattern with feature size of $30\,nm$, we can find that the pattern of mask can be resolved in the photoresist. In fact, the metal have its intrinsic property of absorption which cause the loss of the light travelled along the surface, while the surface plasmons polaritons have its local enhancement. So, we can reasonably apply the both property to transfer the information of the mask to a very long distance. Theoretically, that mean we can apply a lot of metal-dielectric to play the function of lens.
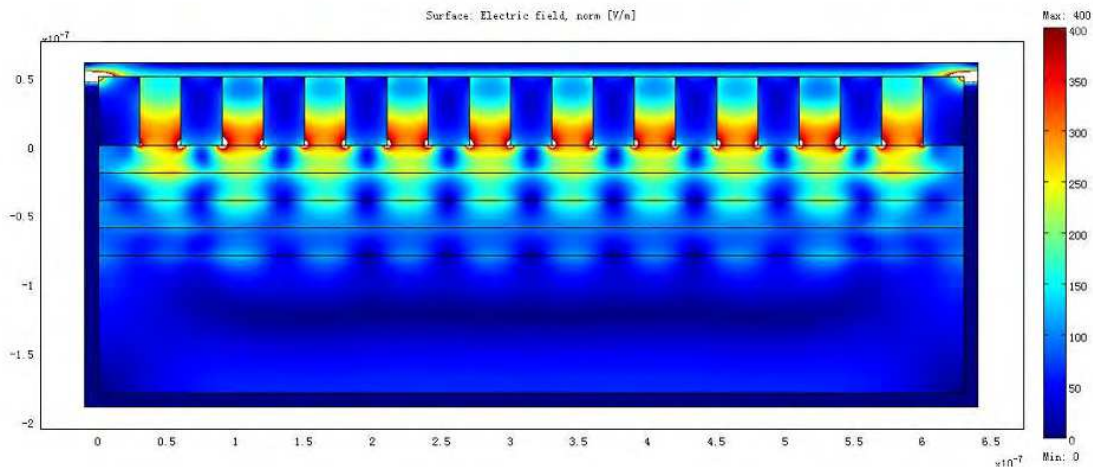

Fig. 9. Electric field distribution of dual-layered hetero-structure for CD=$30\,nm$.

3.6 Nanolithography by dual metal-dielectric hetero-structure

We designed a nanolithography system to demonstrate the technique proposed by the paper, the parameters of our system and the process are shown in Table 2 which is slightly different from the condition of simulation.

Materials	Thickness
Substrate (Quartz)	100nm
Mask (Chromium)	40nm
Spacing (PMMA)	40nm
Silver	30nm
Photoresist (ARP-3170)	100nm
Light Source	i-line (365nm)
Optical Intensity	12.8mW/cm2
Exposure	15s
Development	30s

Table 3. Experiment parameters of our nanolithography system.

The process of our nanolithography should follow a different method from the traditional one. The detailed process is shown in Fig. 9. We should pay special attention to the thickness of each layer during the process. For the precision control of the thickness, it took us a lot of time to finish the process.
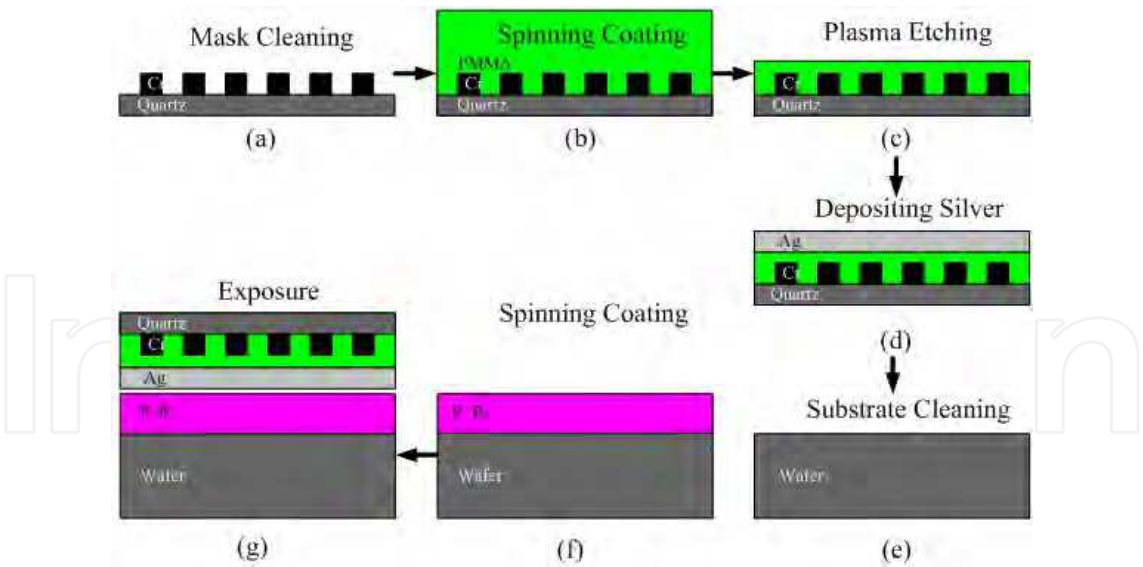

Fig. 10. The special process for the nanolithography.

Fig. 9 is the SEM image of our experiment. It was found that the pattern with feature size of $100\,nm$ has better quality than the pattern with feature size of $50\,nm$ has. As for the pattern with feature size of $50\,nm$, the worse quality may come from the mask fabrication procedure. Because the fabrication of mask with feature size of $50\,nm$ is also a great challenge to FIB or EBL.
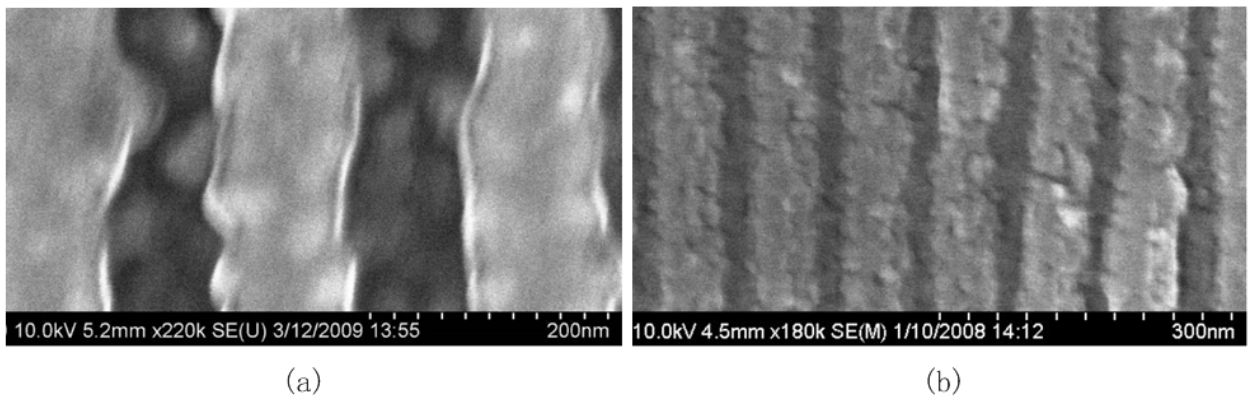
10.0kV 5.2mm x220k SE(U) 3/12/2009 13:55   200nm   10.0kV 4.5mm x180k SE(M) 1/10/2008 14:12   300nm

(a)   (b)

Fig. 11. The experimental results of our nanolithography method. (a) for the feature size of 100 nm and (b) for the feature size of 50 nm .

In brief, the experiment mentioned above demonstrates the feasibility of using noble metal as a special lens which can realize the subwavelength resolution. We believe in that Surface plasmons polaritons will be used as one of the promising tools in the nanometric device and special IC areas for the purpose of high resolution regardless of low yield.

4. Nanolithography by using gain-assisted metamaterials

Seen from equation(3), it seems that there is no other method to reduce the metallic losses to increase the SPPs propagation length in the metal-dielectric configuration.

For the configuration described in Fig. 2, metal got its intrinsic property of absorption; we cannot do anything to metal. However, there seems to be an alternative method to compensate for the losses in the metal. It was reported that if the configuration of metal-dielectric(without gain) was replaced by the configuration of metal-dielectric(with gain), the losses in the metal will be decreased and cause longer propagation length. Based on the report, we proposed a subwavelength optical lithography method which can be simplified in Fig. 9.
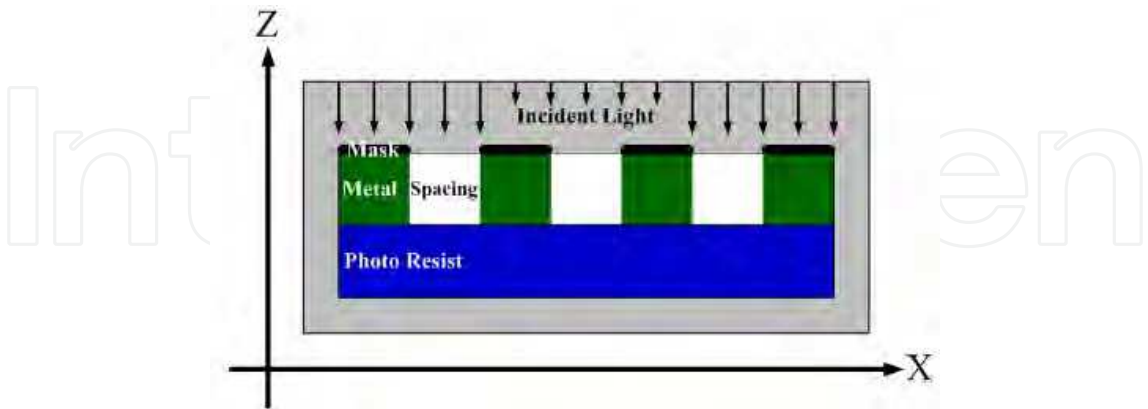

Fig. 12. Sketch of subwavelength optical lithography method.

In Fig. 9, the incident light was introduced to the system with perpendicular direction to the surface; mask acts as an object which blanks the incident light; the photo resist imaged the image of the mask. Due to the diffraction limitation of light, mask with feature size below half wavelength of incident light cannot be resolved by the conventional exposure system.

In our subwavelength optical lithography system, we designed a mask with feature size of $60\,nm$ to demonstrate the resolution of our system. The mask is designed with period of $120\,nm$.

According to the excitation condition of SPPs, once the materials got matched, SPPs will propagate along the interface between metal and dielectric, and we can record the image in photo resist to study the resolving capacity of our subwavelength optical exposure system.

4.1 Computation and analysis

In order to investigate the subwavelength optical lithography method, we pick up the finite element method(FEM) to study the distribution of optical field in photo resist.

The ultraviolet light with wavelength of $365\,nm$ is perpendicular to the surface; the physical parameters of material are shown in Table 3. All the parameters are taken from [Edward D. Palik, Handbook of Optical Constants of Solids. London: Academic Press. 1985] which is highly accepted in optics field.

Materials	Parameters
Mask	ε=-8.8203+i*9.1858
Spacing	ε=2.3013+i*0.0014
Silver	ε=-2.5619+i*0.6015
Photoresist	ε=2.5918+i*0.0097

Table 4. Physical parameters of the materials.

We selected an area of $w \times h = 0.72\mu m \times 0.205\mu m$, as shown in Fig.3, to compute the distribution of optical field when the light with TM mode is introduced into the system. The computation area is surrounded by Perfect Matched Layer(PML) to simplify the simulation process. In order to merely investigate the propagation length of SPPs, we simplified mask with its imaginary part much larger than its real value, which makes mask absorbed most of the incident light to blank the passage. In order to get better results, we picked up higher order of element to carry the computation. In our model, SPPs will propagate along the interface between metal and its surrounding. The size of metal is $w \times h = 0.06\mu m \times 0.06\mu m$.
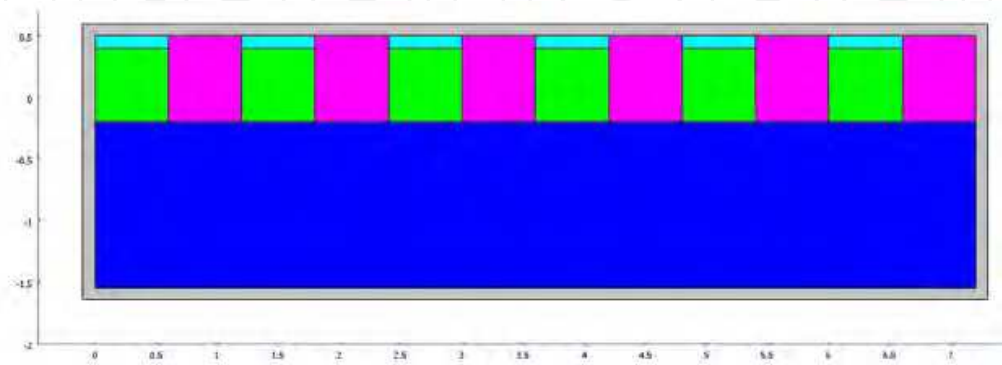

Fig. 13. FEM computation area of model.Fig.3

We chose the electric field to analysis the interaction between photoresist and light which is widely applied in the simulation of optical lithography. Fig. 11(a) and Fig. 11(b) show the distribution of electric filed in our system under ideal condition and real condition, respectively. Both of them show that the SPPs can reach to the exit side of the light passage. The intensity difference caused by the following conditions: in ideal condition, we set the permittivity of metal without no imaginary part, and we made both material perfect matched for the excitation condition of SPPs; in real condition, we set metal with imaginary part, and we made little bit difference between the metal's $\left|\varepsilon_{mR}\right|$ and its surrounding's $\left|\varepsilon_{dR}\right|$ which will cause the excitation condition little mismatched.

In order to investigate the propagation length, we extended the size of metal to $w \times h = 0.06\mu m \times 0.18\mu m$ while other conditions keep fixed as same. Fig. 12(a) and Fig. 12 (b) show the distribution of electric filed in our system under ideal condition and real condition, respectively. Both of them show that the SPPs can reach to the exit side of the passage. For the ideal condition, the enhanced effect in between the passage might be caused by the coupling of SPPs on both surfaces of the passage. Because there is no imaginary part in metal's permittivity, more electromagnetic power can be transferred to the exit surface. However, in the real condition, the uniform distribution was exhibited.
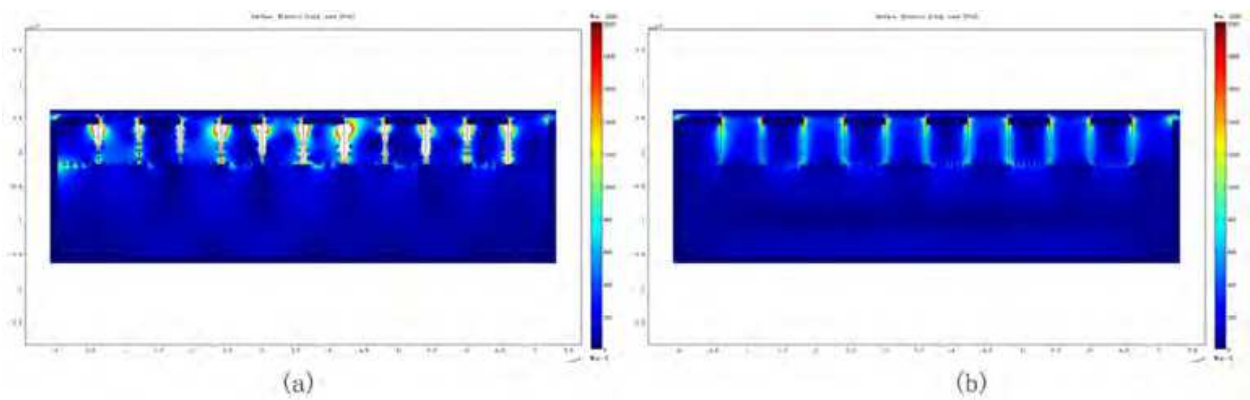

Fig. 14. Distribution of electric filed. (a) for ideal model and (b) for real model.
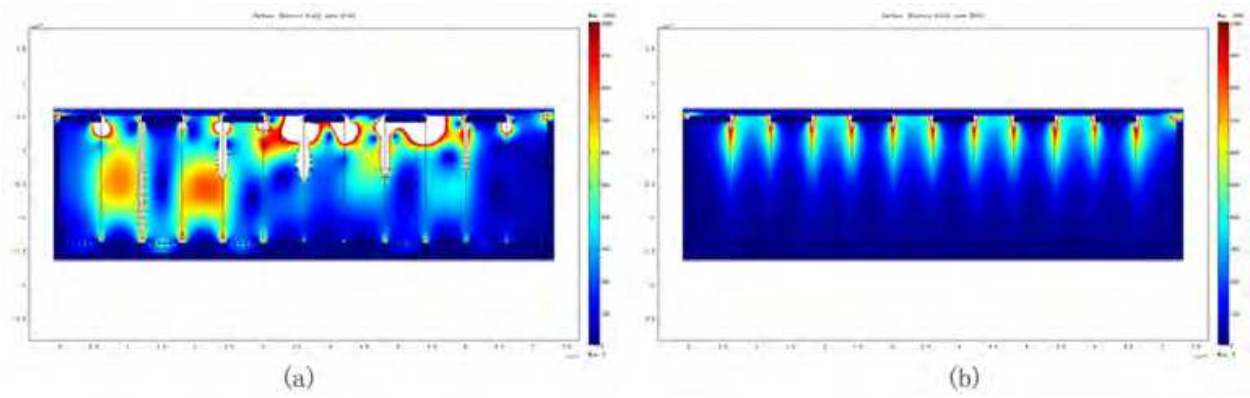

Fig. 15. Distribution of electric filed. (a) for ideal model and (b) for real model.

We pick up the exit surface of the passage to compare the optical lithography result, as shown in Fig. 13(a) and Fig. 13(b). In the both figures, the black solid line and dashed dot line signed for ideal condition and real condition, respectively. Fig. 13(a) and Fig. 13(b)

showed the distribution of the electric field with metal size of $w \times h = 0.06\mu m \times 0.06\mu m$ and $w \times h = 0.06\mu m \times 0.18\mu m$ respectively. We found that the uniformity of real condition is much better than that of ideal condition, which might be caused by the interference among the SPPs on the exit surface.
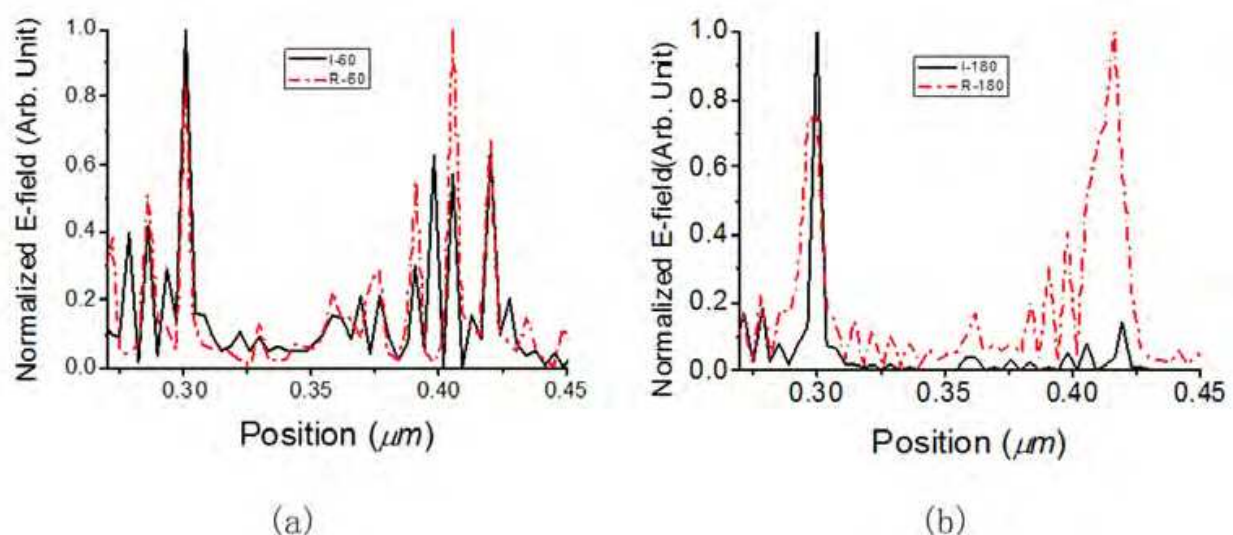

Fig. 16. Distribution of normalized electric filed. (a) for $w \times h = 0.06\mu m \times 0.06\mu m$ and (b) for $w \times h = 0.06\mu m \times 0.18\mu m$.

We investigated the potential propagation length of SPPs on metal-dielectric-metal structure by FEM method. And we demonstrated the subwavelength optical lithography realized by gain-assisted metamaterial. The computation results showed that feature size of $60\,nm$ can be clear resolved by our proposed method. The better resolution can be done by using metamaterials with gain function. Metamaterial showed the special function which can compensate for the intrinsic loses caused by metal.

5. Conclusion

Two types of nanolithography in the evanescent field of noble metal are discussed in this chapter. Both of them focus on the evanescent near field in nano-filmed noble metals. Sub-diffraction-limited feature size can be resolved by using i-line illumination exposure. Better resolution up to $50\,nm$ was successfully simulated and tested in this chapter.

The first applies single or multiple layers of metal-and-dielectric to realize the nanolithography. Nanolithography has been investigated by using optical proximity exposure in the evanescent near field in nano-filmed noble metals. Compared with the model of original superlens, we separated the superlens $100\,nm$ away from the mask, under the illumination of i-line light, the initial simulation shows that the sub-diffraction-limited feature as small as $60\,nm$ line width can be clearly resolved without hard contact between mask and nano-filmed noble metal. By proper design of the materials and the parameters of nano-filmed layers, better resolution can be realized. The experiment showed that pattern with feature size of $50\,nm$ can be reconstructed in the photoresist by our nanolithography method. The experimental results showed the good consistency between the simulation and the experiments. As for the pattern with feature size of $50\,nm$, the worse uniformity of lines

may come from the following aspects: the uniformity of the light source, the worse quality of the mask, the bad precision for the thickness of different layer and the process itself. Anyway, we do believe that we can get better results once we optimize the whole process of the nanolithography.

The second mainly focuses on the gain-assisted metamaterials applied in nanolithography. Surface Plasmon polaritons are electromagnetic waves that propagate along the surface of a conductor, usually a metal. It is shown that the gain-assisted metamaterial can compensate for the intrinsic absorption loss in metal. In this chapter, the propagation of surface plasmon polaritons on gain-assist metamaterial system is investigated. As an example, nanolithography has been considered by using optical proximity exposure in the evanescent near field of gain-assisted metamaterial layer. The evanescent waves carried the detailed information of the object which was defined by the high space frequency of the mask. With the enhancement of surface plasmon polaritons and gain-assisted metamaterials system, the evanescent waves can be propagated to a relatively far distance. Numerical computations by finite element analysis shows that better optimization of the gain-assisted metamaterials system can further improve the resolution. The computation result shows it will be an alternative nanolithography technique for the next generation lithography.

In brief, a plasmonic structure for imaging and super focusing is a new approach besides the concept of negative refractive index. It is possible to realize imaging resolution beyond diffraction limit with a certain working distance within several wavelengths range. To realize this target, one of technical challenges is that how to transfer the high spatial frequency near-field signals from evanescent wave to propagation wave. The other challenge is that how to amplify the near-field evanescent wave from conventional $\sim 180nm$ to be $\sim 1\mu m$ or even several wavelengths in free space.

6. Acknowledgement

7. References

Barnes, W. L., Dereux, A. & Ebbesen, T. W. Surface plasmon subwavelength optics. Nature 424, 824-830 (2003).

D. O. S. Melville, R. J. Blaikie, "Submicro imaging with a planar silver lens", Appl. Phys. Lett. 84(2004)4403.

D. O. S. Melville, R. J. Blaikie, "Super-resolution imaging through a planar silver layer", Optics Express 13(2005)2127.

Edward D. Palik, Handbook of Optical Constants of Solids. London: Academic Press. 1985.

Guanxiao Cheng, Chao Hu, Ping Xu, and Tingwen Xing, "Zernike apodized photon sieves for high-resolution phase-contrast x-ray microscopy," *Opt. Lett.* 35, 3610-3612 (2010).

Guanxiao Cheng, Tingwen Xing, Wumei Lin, Jinmei Zhou, Chuankai Qiu, Zhijie Liao, Yong Yang, Lei Hong, Jianling Ma, "Photon sieve array x-ray maskless nanolithography," *Proc. SPIE* 6517, 651736 (2007).

Guanxiao Cheng, Tingwen Xing, Yong Yang, Jianling Ma, "Experimental characterization of optical properties of photon sieve," *Proc. SPIE* 6724, D7240 (2007).

Guanxiao Cheng, Tingwen Xing, Yong Yang, Jianling Ma, "Resolution enhancement of photon sieve based on apodization", *Proc. SPIE* 6832, 83229 (2008).

Heinz Raether. Surface Plasmons on Smooth and Rough Surfaces and on Gratings. New York: Springer-Verlag.

J.B. Pendry, "Negative refraction makes a perfect lens", Physical Review Letters, Vol.85, No.18 (2000).

J.G. Goodberlet, H. Kavak, "Patterning sub-50nm features with near-field embedded-amplitude masks", Appl. Phys. Lett. 81 (2002) 1315.

Lezec, H. J. et al. Beaming light from a subwavelength aperture. Science, 2002(107): 1895.

M.M. Alkaisi, R.J. Blaikie, S.J. McNab, R. Cheung, D.R.S. Cumming, "Sub-fiffracion-limited patterning using evanescent near-field optical lithography", Applied Physics Letters, Vol.75, No.22(1999).

Maziar P. Nezhad, Kevin Tetz, Yeshaiah Fainman. Gain assisted propagation of surface Plasmon polaritons on planar metallic waveguides. Optics Express, Vol.12 No. 17(2005): 4072-4079

Nicholas Fang, Hyesog Lee, Cheng Sun, Xiang Zhang, "Sub-diffraction-limited optical imaging with a silver superlens", Science, Vol. 308(2005).

Ritchie, R. H. Plasma losses by fast electrons in thin films. Phys. Rev., 1957(106):874-881

Shaolin zhou, Feng Xu, Song Hu, Xiaoping Tang, "Positioning scheme based on Grating modulation and phase imaging in lithography", Proc. SPIE, the 5th International Symposium on Advanced Optical Manufacturing.

Shaolin Zhou, Yong Yang, Lixin Zhao, and Song Hu, "Tilt-modulated spatial phase imaging method for wafer-mask leveling in proximity lithography" Opt. Lett. 35, 3132-3134(2010).

Shaolin Zhou, Yongqi Fu, Xiaoping Tang, S. Hu, Wangfu Chen, and Yong Yang, "Fourier-based analysis of moiré fringe patterns of superposed gratings in alignment of nanolithography," Opt. Express 16, 7869-7880 (2008).

T. W. Ebbesen, H. J. Lezec, H. F. Ghaemi, T. Thio, and P. A. Wolff, Extraordinary optical transmission through sub-wavelength hole array, Nature 391, 667-669 (1998).

W. L. Barnes, W. A. Murray, J. Dintinger, E. Devaux, T. W. Ebbesen. Surface Plasmon polaritons and their role in the enhanced transmission of light through periodic arrays of subwavelength holes in a metal film. Phys. Rev. Lett., 2004(92): 107401

Xiangang Luo, Teruya Ishihara, "Surface Plasmon resonant interference nanolithography technique", Applied Physics Letters, Vol. 84, No.23 (2004).

Yong Yang, Hanmin Yao, Song Hu, Guanxiao Cheng, "Nanolithography in the evanescent field by using silver layer", Proc. SPIE 6724, 77241A(2007).

Yong Yang, Song Hu, Hanmin Yao, Guanxiao Cheng, Chunmei Zhang, Wei Yan, "Nanolithography in the Evanescent Near Field by Using Nano-filmed Noble Metal Layers," *Proc. SPIE* 6724, 77241A (2007).

Yong Yang, Yongqi Fu, Hanmin Yao, Song Hu, Shaolin Zhou, Wei Yan, Wangfu Chen, Guanxiao Cheng, Zhan Li, "Beam Splitter Achieved by Using Metallic Structure with Nanoslits," *J. Comput. Theor. Nanosci.* 6(5),1030-1033,(2009).
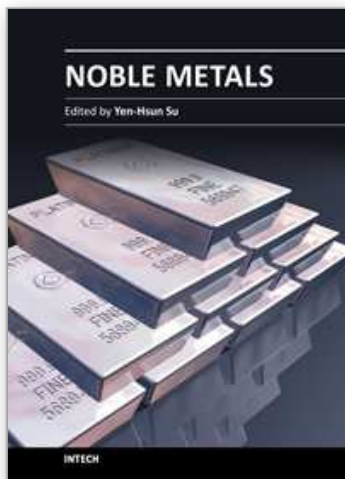
Noble Metals

Edited by Dr. Yen-Hsun Su

ISBN 978-953-307-898-4

Hard cover, 426 pages

Publisher InTech

Published online 01, February, 2012

Published in print edition February, 2012

This book provides a broad spectrum of insights into the optical principle, resource, fabrication, nanoscience, and nanotechnology of noble metal. It also looks at the advanced implementation of noble metal in the field of nanoscale materials, catalysts and biosystem. This book is ideal not only for scientific researchers but also as a reference for professionals in material science, engineering, nonascience and plasmonics.

How to reference

In order to correctly reference this scholarly work, feel free to copy and paste the following:

Yong Yang, Guanxiao Cheng, Shaolin Zhou, Lixin Zhao and Song Hu (2012). Nanolithography in the Evanescent Field of Noble Metals, Noble Metals, Dr. Yen-Hsun Su (Ed.), ISBN: 978-953-307-898-4, InTech, Available from: http://www.intechopen.com/books/noble-metals/nanolithography-in-the-evanescent-field-of-noble-metals

INTECH
open science | open minds